

Body Composition Profiling in the UK Biobank Imaging Study

Jennifer Linge¹, Magnus Borga^{1,2,3}, Janne West^{1,2,4}, Theresa Tuthill⁵, Melissa R. Miller⁶, Alexandra Dumitriu⁶, E. Louise Thomas⁷, Tobias Romu^{1,2,3}, Patrik Tunón¹, Jimmy D. Bell⁷, and Olof Dahlqvist Leinhard^{1,2,4}

Objective: This study aimed to investigate the value of imaging-based multivariable body composition profiling by describing its association with coronary heart disease (CHD), type 2 diabetes (T2D), and metabolic health on individual and population levels.

Methods: The first 6,021 participants scanned by UK Biobank were included. Body composition profiles (BCPs) were calculated, including abdominal subcutaneous adipose tissue, visceral adipose tissue (VAT), thigh muscle volume, liver fat, and muscle fat infiltration (MFI), determined using magnetic resonance imaging. Associations between BCP and metabolic status were investigated using matching procedures and multivariable statistical modeling.

Results: Matched control analysis showed that higher VAT and MFI were associated with CHD and T2D ($P < 0.001$). Higher liver fat was associated with T2D ($P < 0.001$) and lower liver fat with CHD ($P < 0.05$), matching on VAT. Multivariable modeling showed that lower VAT and MFI were associated with metabolic health ($P < 0.001$), and liver fat was nonsignificant. Associations remained significant adjusting for sex, age, BMI, alcohol, smoking, and physical activity.

Conclusions: Body composition profiling enabled an intuitive visualization of body composition and showed the complexity of associations between fat distribution and metabolic status, stressing the importance of a multivariable approach. Different diseases were linked to different BCPs, which could not be described by a single fat compartment alone.

Obesity (2018) **26**, 1785-1795. doi:10.1002/oby.22210

Introduction

Anthropometric measures, such as BMI, are poor predictors of body fat distribution and associated metabolic risk, particularly at an individual level (1-3). Moving toward individualized medicine, specific measures of body composition could greatly advance our understanding of obesity, metabolic health, aging, and chronic diseases. Magnetic resonance imaging (MRI) is extensively used for body composition analysis (2,4-7) and is accepted as the gold standard in body composition research (4,8). Recently developed MRI techniques allow for advanced body composition profiling and phenotyping using standardized acquisition protocols, enabling a comparison of measurements across large-scale cohorts and between different studies (7,9). The use of these techniques enables separation of fat and muscle compartments from a single 6- to 10-minute MRI examination with a high success rate (7).

Ectopic fat accumulation in various compartments of the body is a hallmark of metabolic syndrome and related comorbidities (10,11). Increased visceral adipose tissue (VAT) is related to increased cardiac risk (12-14,16), type 2 diabetes (T2D) (15,16), liver inflammation and fibrosis (17), and certain types of cancer (18,19). Increased intramuscular adipose tissue, or muscle fat infiltration (MFI), has been associated with reduced mobility (20) and increased risk for T2D (21). Moreover, increased liver fat may lead to advanced fibrosis, cirrhosis, and hepatocellular carcinoma (22,23), and it is also linked to the development of T2D (22,24).

To understand the development of metabolic diseases, investigations of the interplay between several different adipose tissue compartments are needed. Although most adipose tissue compartments are correlated with general adiposity and BMI, disease risks tend to be related to specific patterns or balance in fat accumulation (2,12). To further our understanding

¹ AMRA Medical AB, Linköping, Sweden. Correspondence: Jennifer Linge (jennifer.linge@amramedical.com) ² Centre for Medical Image Science and Visualization, Linköping University, Linköping, Sweden ³ Department of Biomedical Engineering, Linköping University, Linköping, Sweden ⁴ Department of Medical and Health Sciences, Linköping University, Linköping, Sweden ⁵ Imaging, Precision Medicine, Pfizer Inc., Cambridge Massachusetts, USA ⁶ WRD Genome Sciences & Technologies, Pfizer Inc., Cambridge, Massachusetts, USA ⁷ Research Centre for Optimal Health, School of Life Sciences, University of Westminster, London, UK.

Funding agencies: This research was supported by Pfizer Inc.

Disclosure: MB, JW, TR, PT, and ODL are stockholders in and employees of AMRA Medical AB. JL is an employee of AMRA Medical AB. JL, MB, JW, TR, PT, and ODL report funding support from Pfizer Inc. during the conduct of the study. JL, MB, and ODL have a patent evaluating an individual's characteristics of at least one phenotype variable pending. TT, MRM, and AD are employees of Pfizer Inc. JDB and ELT declared no conflict of interest.

Additional Supporting Information may be found in the online version of this article.

Received: 12 March 2018; **Accepted:** 17 April 2018; **Published online** 22 May 2018. doi:10.1002/oby.22210

This is an open access article under the terms of the Creative Commons Attribution-NonCommercial-NoDerivs License, which permits use and distribution in any medium, provided the original work is properly cited, the use is non-commercial and no modifications or adaptations are made.

of the complex interplay between muscle metabolism, adipose tissue accumulation, and ectopic fat, more refined tools are needed.

The aims of this study were to investigate the value of multivariable body composition profiling, by relating the individual body composition profile (BCP) to population scale data from the UK Biobank imaging cohort (25), and to describe the specific associations with diagnosed coronary heart disease (CHD), T2D, and metabolic health by utilizing an intuitive multidimensional visualization.

Methods

Subjects

The first 6,021 participants from the UK Biobank imaging substudy were included, with a mean age of 62.3 ± 7.5 (44.6–78.3) years and a BMI of 26.7 ± 4.4 (16.0–58.0) kg/m². The UK Biobank is a population-based study enrolled in 2006, following 502,682 participants, with the aim to improve the prevention, diagnosis, and treatment of a wide range of serious and life-threatening illnesses. Baseline assessment gathered extensive information via physical measurements, questionnaires, samples, and consent to access medical records. Following baseline assessment, 100,000 participants are being recalled for an imaging study of the brain, heart, bones, carotid arteries, and body composition, as well as a repeat of the baseline assessment (26). This research has been conducted using the UK Biobank resource, project ID 6569. The study was approved by the North West Multicenter Research Ethics Committee in the United Kingdom. Written informed consent was obtained prior to study entry.

MRI scanning

The subjects were scanned in a Siemens MAGNETOM Aera 1.5-T MRI scanner (Siemens Healthineers, Erlangen, Germany) using a 6-minute dual-echo Dixon Vibe protocol, providing a water and fat separated volumetric data set covering neck to knees, and a single-slice multiecho Dixon acquisition for proton density fat fraction (PDFF) assessment in the liver. For body composition, acquired image data were analyzed for VAT, abdominal subcutaneous adipose tissue (ASAT), thigh muscle volume, MFI in the anterior thighs, and liver PDFF. Briefly, the image analysis consisted of (1) image calibration, (2) fusion of image stacks, (3) image segmentation, and (4) quantification of fat and muscle volumes (7,9,27–29) and included manual quality control by an analysis engineer. Body composition analyses were performed using AMRA Profiler Research (AMRA Medical AB, Linköping, Sweden). The online Supporting Information provides detailed information of *in vivo* acquisitions and analysis.

Body composition profiling

A BCP was defined as a combination of variables that together describe the fat and/or muscle distribution of an individual or group. When applying statistical modeling, the following BCP variables describing adipose tissue distribution throughout the body without physically overlapping each other were used: VAT index (VATi), or VAT normalized by height squared to compensate for subject size (30); ASAT index (ASATi), or ASAT normalized by height squared; liver PDFF; and MFI. When visualizing body composition, the six-axis BCP plot was used (Figure 1).

Visualizing BCP

The variables used in the BCP plot jointly describe fat accumulation and fat and muscle distribution, and they allow for a quick assessment of body composition based on the shape in the BCP plot. Specifically, the visualization illustrates the balance between different adipose tissue compartments and the distribution of fat, diffuse fat infiltration, and muscles in the body. It comprises VATi; total abdominal adipose tissue index (TAATi), which is the total abdominal fat (VAT + ASAT) normalized by height squared, a fat-specific version of BMI; weight-to-muscle ratio (WMR), which is body weight divided by thigh muscle volume, indicating the ability of subjects to carry their weight; fat ratio (FR), which is the total abdominal fat divided by total abdominal fat and thigh muscle volume, assessing the distribution between fat and muscle volume; MFI; and liver PDFF.

The BCP plot displays multivariable data in a six-axis radar chart (Figure 1). Because of the difference in magnitude and distribution between the BCP variables, they were mapped using a logarithmic sigmoid transfer function (Figure 2) with distribution-specific constants to values between 0 (chart center) and 1 (end of spokes). The same type of transfer function, with the median values of a metabolic disease-free (MDF) group as references, was used for all variables. To align the distribution-specific constants and reference values in the radar chart, and therefore level the visual response between variables, they were mapped to fixed distances from the chart center. The reference values were mapped to 0.15 for variables with only ectopic fat (liver PDFF, VATi, and MFI) and to 0.6 for the remaining variables, forming the shape of a star (Figure 1A). Changes in variables on axes with only ectopic fat dominated the appearance of the resulting BCP (i.e., highlighting the ectopic fat compartments). An individual was visualized with a line (Figure 1B) and a group with a shaded field covering the interquartile range (Figure 1C–1D).

Stratification of metabolic subgroups

Diagnosis information was gathered through inpatient electronic health care records (downloaded November 2016, available from 1995–2015) and via touch screen questionnaires followed by interviews performed by trained nurses.

Metabolic disease free. To identify subjects asymptomatic of metabolic diseases, a list of conditions considered to be serious enough to represent metabolically focused health concerns (e.g., cardiovascular and metabolic diseases, severe chronic conditions, neurological diseases, cancers) (Supporting Information Table S1), reviewed by an experienced clinician, was used. Participants were considered MDF if they did not report any of the listed diseases (UK Biobank field identification numbers 20001 and 20002) (31) and if they did not have the *International Classification of Diseases, 10th Revision* (ICD-10) codes mapping to strings similar to the listed diseases (supplementary file by Neuraz et al. used for mapping) (32).

CHD

- Cases—Data from the electronic health care records only were used to identify subjects with diagnosed CHD. Subjects with ischemic heart disease or presence of aortocoronary bypass graft (ICD-10 codes I20–I25, Z951) were considered CHD cases.
- Controls—CHD controls did not have any of the above ICD-10 codes. In addition, they had no self-reported history of heart attack, angina, other heart and/or cardiac problems, or diabetes diagnosed by a

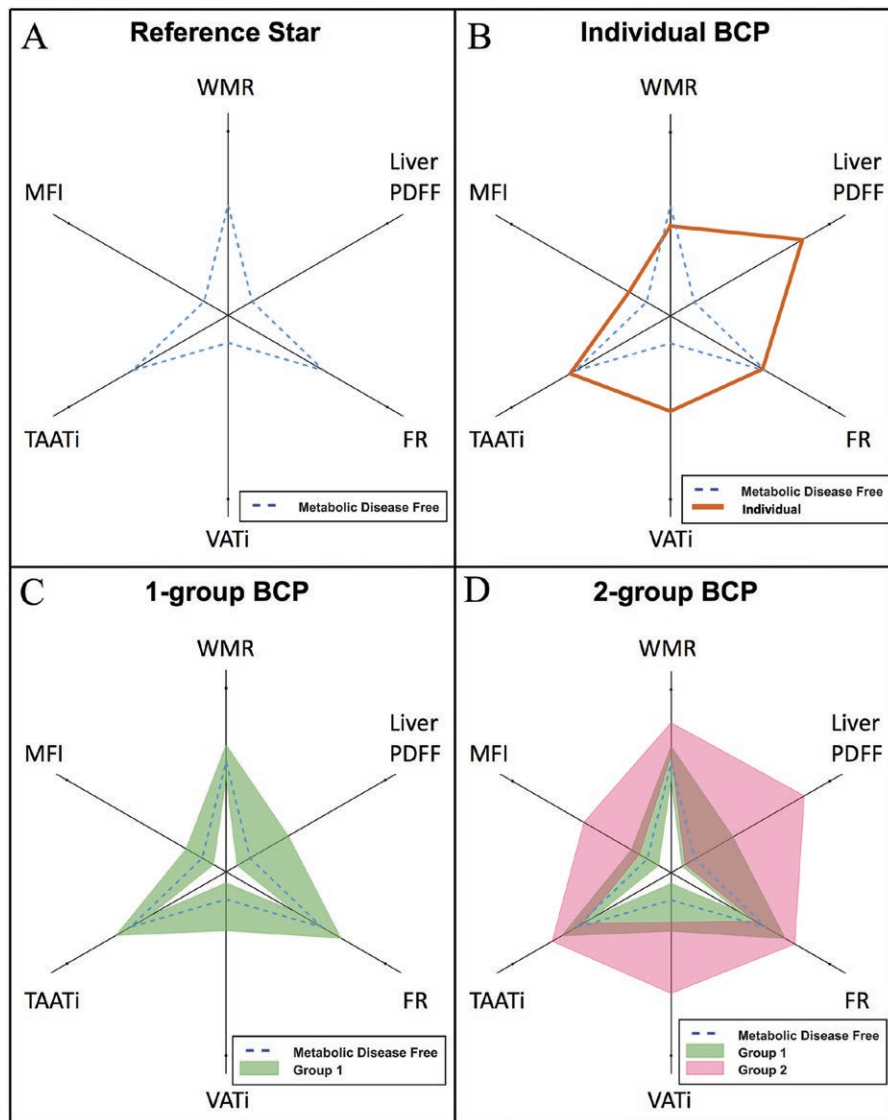


Figure 1 Visualization examples of the body composition profile (BCP). (A) Median of a metabolic disease-free (MDF) population (same in B-D); (B) an individual BCP (orange); (C) a group visualized as the field spanning the interquartile range (green); (D) two groups visualized as fields spanning their interquartile ranges (green and pink); brown areas represent the overlap between groups. FR, fat ratio; MFI, muscle fat infiltration; PDFF, proton density fat fraction; TAATi, total abdominal adipose tissue index; VATi, visceral adipose tissue index; WMR, weight-to-muscle ratio.

doctor. Supporting Information Table S2 lists fields used for stratification. Statistical analyses excluded subjects not characterized as CHD cases or controls ($n=1,384$).

T2D

- Cases—Subjects with diabetes diagnosed by a doctor and an age of diagnosis of 30 years or older were considered T2D cases.
- Controls—Subjects with diabetes diagnosed by a doctor and an age of diagnosis younger than 30 years, or with gestational diabetes,

were excluded from the T2D controls. Supporting Information Table S3 lists fields used for stratification. Statistical analysis excluded subjects not characterized as T2D cases or controls ($n=38$).

Matched controls. For CHD and T2D, two matched control groups were stratified matched on (1) sex and age and (2) sex, age, and BMI. Each control was chosen as the nearest neighbor with the same sex in the euclidean space constructed by (1) age and (2) normalized (standard score normalization) age and BMI.

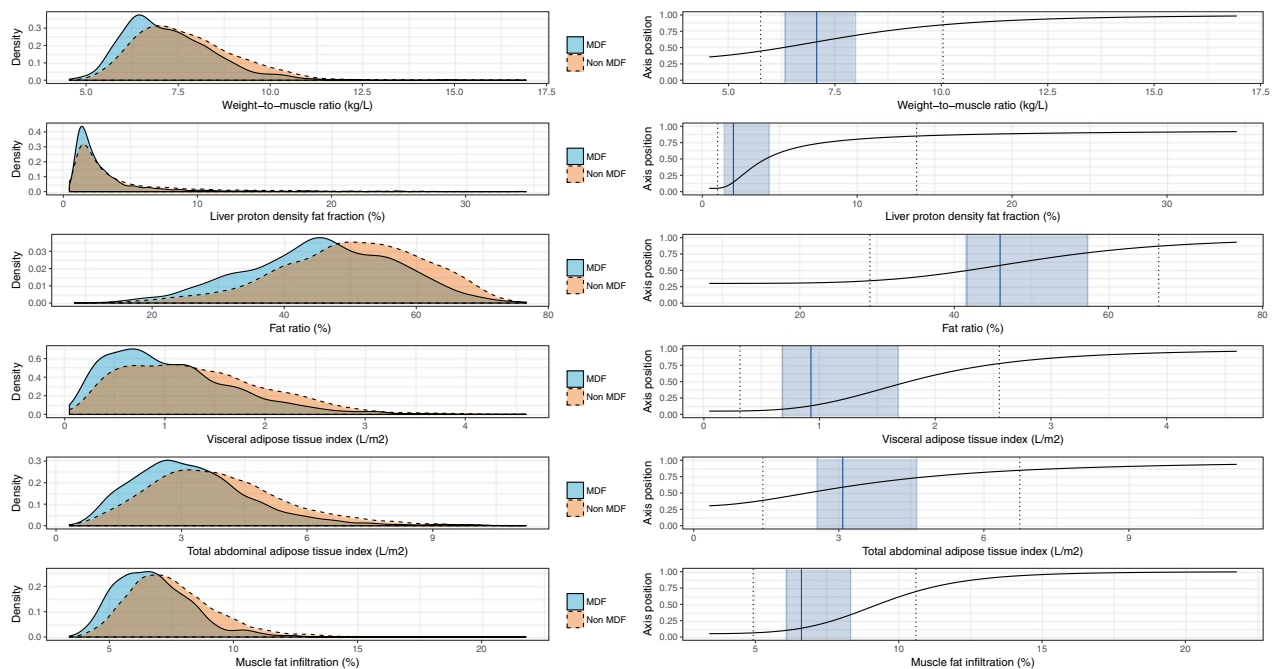


Figure 2 Density and scaling of BCP variables. Left panels are the density plots for each BCP variable comparing MDF subjects (solid contour) with those not characterized as MDF (dashed contour); right panels are the transfer functions from BCP variable values to their position on corresponding axes in the BCP plot, including median values (solid line) and the interquartile ranges (shaded areas) of the MDF group as reference and the 5th and 95th percentile of the whole cohort (dashed lines). BCP, body composition profile; MDF, metabolic disease free. [Colour figure can be viewed at wileyonlinelibrary.com]

Cases had controls selected by repeating the following: (1) exclude controls with opposite sex, (2) choose the closest control, and (3) remove that control from remaining controls.

Acquisition and definition of covariates

Height was recorded using a Seca 240 height measure (Seca, Hamburg, Germany), and weight was recorded with a Tanita BC-418MA body composition analyzer (Tanita Corp., Arlington Heights, Illinois). Smoking status, alcohol intake, physical activity, and statin medication were derived using data from touch screen questionnaires and/or interviews (see Supporting Information for further details).

Statistical analysis

Individual assessment. Two multivariable logistic regression models were used to investigate each individual's association to CHD, T2D, and MDF, including (1) sex and age and (2) sex, age, and BCP (VAT_i, ASAT_i, liver PDFF, and MFI). To adjust for the sex and age dependence in the disease prevalence data, a sex-and-age normalized predicted probability was calculated. Each predicted probability, calculated using the log odds from the model outputs including BCP, was divided by that from the model including only sex and age. Subjects from three BMI intervals, 24 (23-25) (normal weight), 28 (27-29) (overweight), and 32 (31-33) (obesity), all approximately 65 years old, were used to exemplify.

Group assessment. The CHD and T2D subgroups were visualized in BCP plots. The statistical significance of differences in the BCP variables between cases and controls was tested using the nonparametric Mann-Whitney *U* test ($P < 0.05$ significant).

Statistical modeling. Multivariable logistic regression models were also used to investigate the association of CHD, T2D, and MDF to BCP (VAT_i, liver PDFF, MFI, and ASAT_i), including potential confounding effects of sex and age (Model MV), smoking status, alcohol intake, and physical activity (Model MV + lifestyle), and BMI (Model MV + lifestyle + BMI). Liver PDFF was Box-Cox transformed ($\lambda = -0.51$). All models were run for the whole cohort, males and females separately, with and without statin treatment adjustment.

Post hoc analysis. For CHD, the group assessment was extended by comparison with a control group matched on sex, age, and VAT_i. Computations were performed using R version 3.4.0 (The R Foundation, Vienna, Austria). The Supporting Information lists additional R packages.

Results

Descriptive characteristics

Table 1 summarizes the characteristics of all participants, males, females, and MDF subjects. Among females, 85.2% had menopause or had undergone a hysterectomy.

TABLE 1 Descriptive characteristics of overall participants, males, and females

	Whole cohort	Males	Females	Metabolic disease free
N subjects	6,021	2,864	3,157	1,996
Age, y	63.15 (56.47-68.15)	64.29 (57.44-68.74)	62.35 (55.84-67.50)	60.26 (53.72-66.09)
Sex, male/female	2,864/3,157	2,864/0	0/3,157	928/1,068
Coronary heart disease, %	3.9	5.8	2.3	0
Type 2 diabetes, %	4.6	6.5	3.0	0
Metabolic disease free, %	33.2	32.4	33.8	100
Weight, kg	75.00 (65.50-85.70)	82.80 (75.00-91.50)	67.40 (60.50-76.10)	72.90 (64.00-83.50)
BMI, kg/m²	26.14 (23.63-29.04)	26.75 (24.52-29.28)	25.38 (22.87-28.76)	25.36 (23.17-28.11)
Physical activity, MET-min/wk	3,519.75 (1,804.33-6,002.62)	3,817.97 (2,022.56-6,445.19)	3,222.00 (1,635.16-5,620.94)	3,766.25 (2,046.59-6,349.69)
Smoking status, never/previous/ current	3,594/2,093/262	1,595/1,086/152	1,999/1,007/110	1,277/598/95
Alcohol intake, g/d	15.80 (6.75-27.92)	20.15 (10.53-35.73)	11.57 (5.27-21.06)	15.80 (7.90-27.71)
Statins medication, %	20.61	28.87	13.11	4.65
Visceral adipose tissue, L	3.32 (1.94-5.03)	4.62 (3.25-6.38)	2.33 (1.46-3.51)	2.78 (1.64-4.30)
Abdominal subcutaneous adipose tissue, L	6.44 (4.77-8.65)	5.50 (4.27-7.06)	7.50 (5.57-9.93)	5.94 (4.39-8.04)
Thigh muscle volume, L	9.87 (8.14-12.27)	12.39 (11.23-13.53)	8.23 (7.49-9.06)	9.94 (8.16-12.40)
Weight-to-muscle ratio, kg/L	7.43 (6.63-8.43)	6.68 (6.22-7.23)	8.25 (7.53-9.13)	7.18 (6.41-8.13)
Liver proton density fat fraction, %	2.34 (1.47-4.55)	2.87 (1.74-5.67)	1.96 (1.32-3.69)	2.04 (1.38-3.57)
Fat ratio, %	50.14 (42.24-57.76)	45.76 (38.89-51.62)	55.35 (47.35-61.74)	47.24 (39.49-55.04)
Visceral abdominal adipose tissue index, L/m²	1.17 (0.71-1.72)	1.52 (1.05-2.07)	0.89 (0.55-1.33)	0.99 (0.60-1.46)
Abdominal subcutaneous adipose tissue index, L/m²	2.23 (1.63-3.14)	1.78 (1.38-2.29)	2.87 (2.10-3.78)	2.06 (1.47-2.90)
Total abdominal adipose tissue index, L/m²	3.57 (2.61-4.69)	3.38 (2.53-4.32)	3.82 (2.72-5.08)	3.18 (2.35-4.17)
Muscle fat infiltration, %	7.19 (6.18-8.42)	6.66 (5.73-7.77)	7.67 (6.66-8.88)	6.79 (5.79-7.86)

For continuous variables, median and interquartile range shown.
 MET, metabolic equivalents.

Statistical analysis

Individual assessment. Figure 3 exemplifies individual BCP assessments with sex-and-age normalized predicted probabilities for CHD, T2D, and MDF in bar plots. Females were used to exemplify. Supporting Information Figure S1 shows the results for males. The predicted probabilities for CHD and T2D did not covary, i.e., within all BMI ranges, subjects exhibited different combinations of the following predicted probabilities for CHD and T2D: low-low, high-low, low-high, and high-high. Among subjects with overweight and obesity, there were those exhibiting lower predicted probability for disease compared with subjects with normal weight.

Group assessment. CHD and T2D cases showed significantly higher values for all BCP plot variables ($P < 0.001$) compared with all controls (Figure 4; Table 2). Comparing CHD cases with sex-and-age matched controls, all variables except liver PDFF had significantly higher values ($P < 0.001$). Comparison with sex, age, and BMI matched controls showed significantly higher values in VATi ($P < 0.05$) only. Comparison with sex, age, and VATi matched controls (post hoc analysis) showed significance in liver PDFF only. Liver PDFF was

lower among CHD cases (2.69% [1.64-7.39%] median, interquartile range) compared with controls (3.64% [2.04-7.20%]; $P < 0.05$).

Comparing T2D cases with sex-and-age matched controls, all variables had significantly higher values ($P < 0.001$). Comparison with sex, age, and BMI matched controls showed significantly higher values for WMR, VATi, liver PDFF, and MFI ($P < 0.05$). Differences in FR and TAATi were nonsignificant.

Statistical modeling. Figure 5 presents multivariable logistic regression results showing associations of CHD, T2D, and MDF with BCP for the whole cohort as well as males and females separately. CHD had a positive association to VATi when applying multivariable statistical modeling to the whole cohort ($P < 0.001$), males only ($P < 0.001$), and females only ($P = 0.013$), adjusted for sex (whole cohort) and age (Model MV). Associations remained significant after adjustment for lifestyle factors (smoking status, alcohol intake, and physical activity; Model MV+lifestyle) and BMI (Model MV+lifestyle+BMI) and statin treatment. MFI was positively associated with CHD for the whole cohort ($P = 0.018$), when adjusting for sex and age and when applying

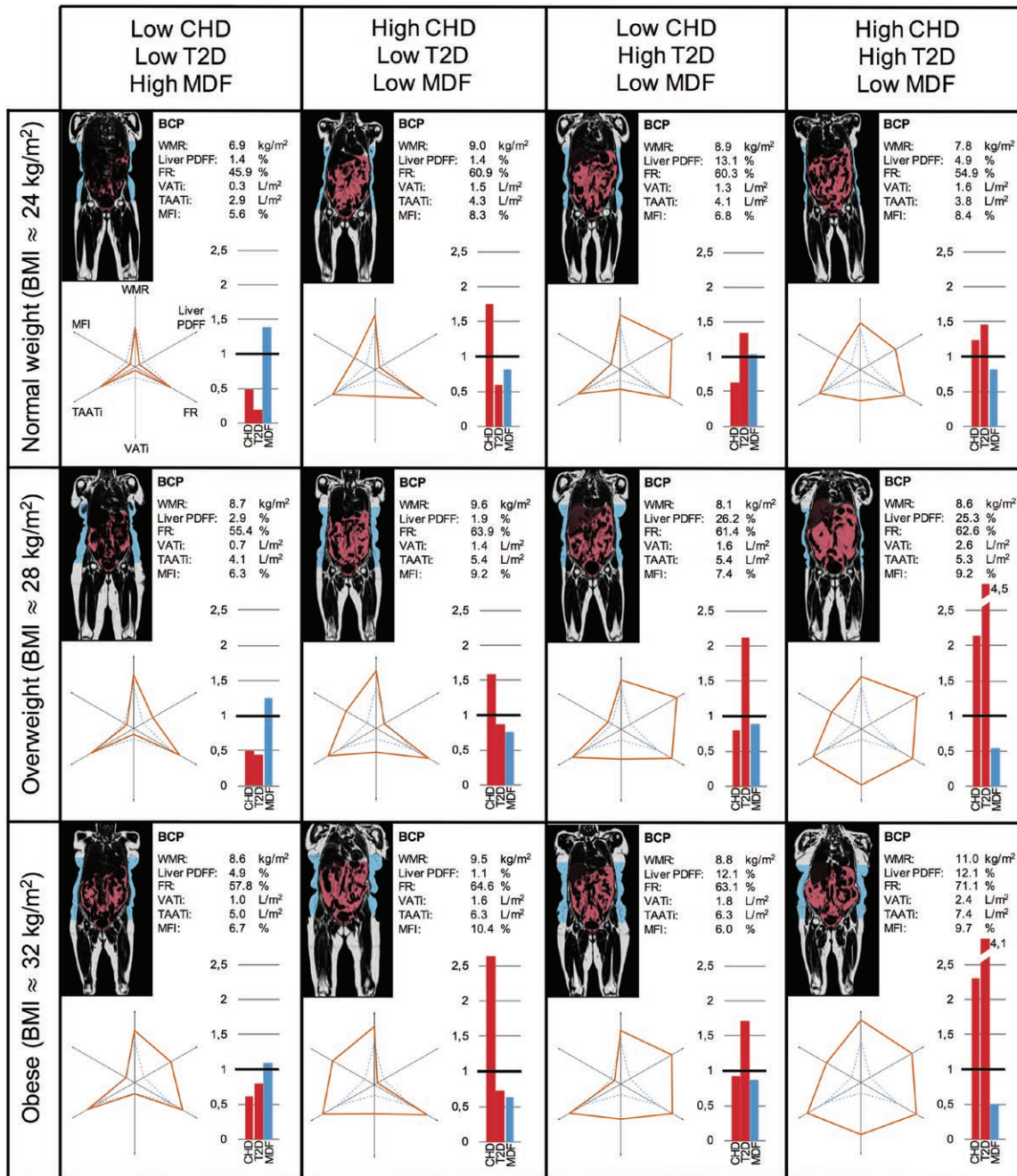


Figure 3 Body composition profiling of females from the UK Biobank imaging cohort. Each subject, approximately age 65, is presented with a coronal slice from the MRI scan with VAT (red) and ASAT (blue) segmentations, the BCP values with corresponding six-axis plots, and bar plots showing sex-and-age normalized predicted probabilities. BCP, body composition profile; CHD, coronary heart disease; FR, fat ratio; MDF, metabolic disease free; MFI, muscle fat infiltration; ASAT, abdominal subcutaneous adipose tissue; PDFF, proton density fat fraction; T2D, type 2 diabetes; TAAATi, total abdominal adipose tissue index; VATi, visceral adipose tissue index; WMR, weight-to-muscle ratio. [Colour figure can be viewed at wileyonlinelibrary.com]

all adjustments (Models MV+lifestyle and MV+lifestyle+BMI), except for statin treatment. In the females only model, MFI was significantly higher when adjusting for age ($P=0.022$) (Model MV). In the male model, MFI was nonsignificant. Liver PDFF was negatively associated with CHD for the whole cohort ($P=0.004$) and in males

($P<0.001$) adjusting for sex (whole cohort) and age. Associations remained significant applying all adjustments (Models MV+lifestyle and MV+lifestyle+BMI), including statin treatment. The association between liver PDFF and CHD in the female model was nonsignificant. ASATi was nonsignificant in all models.

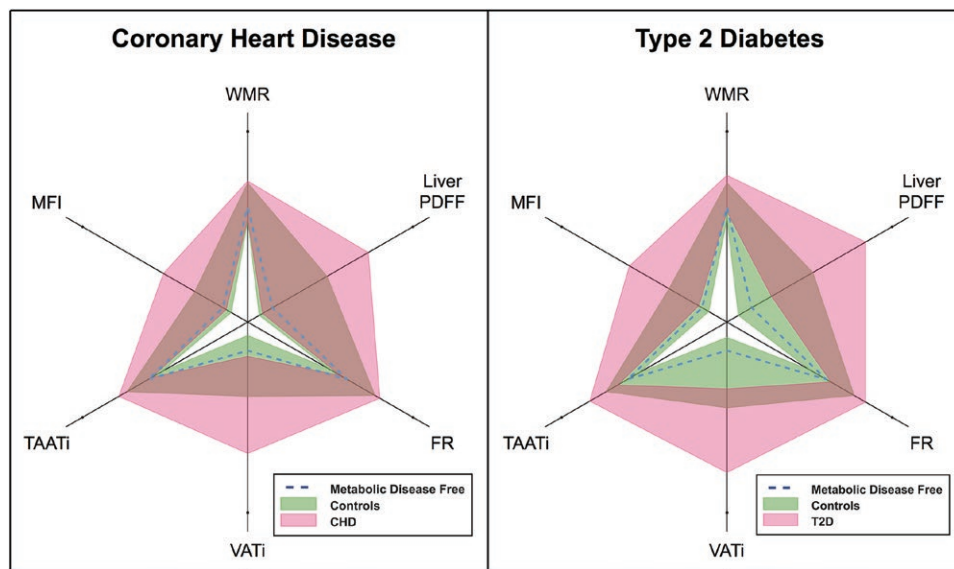


Figure 4 Body composition profiling of coronary heart disease and type 2 diabetes. Pink and green fields represent the interquartile ranges of cases and controls, respectively, brown areas the overlap between groups, and dashed blue lines the median of a metabolic disease-free group as reference. FR, fat ratio; PDFF, proton density fat fraction; MFI, muscle fat infiltration; T2D, type 2 diabetes; TAATi, total abdominal adipose tissue index; VATi, visceral adipose tissue index; WMR, weight-to-muscle ratio. [Colour figure can be viewed at wileyonlinelibrary.com]

T2D was associated with higher VATi, liver PDFF, and MFI adjusting for sex (whole cohort) and age (all $P < 0.01$) (Model MV). Associations remained significant after applying all adjustments (Models MV + lifestyle and MV + lifestyle + BMI), including statin treatment. ASATi was nonsignificant.

MDF was associated with lower VATi for the whole cohort ($P < 0.001$), males only ($P < 0.001$), and females only ($P = 0.013$), adjusting for sex (whole cohort) and age, and lower MFI (all $P < 0.02$), adjusting for sex (whole cohort) and age (Model MV). Liver PDFF was nonsignificant. Associations remained significant after applying all adjustments (Models MV + lifestyle and MV + lifestyle + BMI), including statin treatment. ASATi was significant in the male model including BMI ($P = 0.045$).

Discussion

This study examined the effectiveness of multivariable, MRI-based body composition profiling to further our understanding of metabolic health. Investigating the associations between CHD and T2D and each fat compartment separately (Table 2) showed positive associations with most of the fat compartments. Matching on BMI left only VATi with a significant association to CHD, while matching on VATi instead of BMI showed a significant negative association to liver PDFF. This result was also reflected in the whole cohort and among males when applying statistical modeling including multiple fat compartments (Figure 5). Low ectopic fat, especially VATi and MFI, was positively associated with metabolic health, and higher values were found among subjects with metabolic diseases (Table 2; Figure 4 and Figure 5), while liver PDFF had no significant association. The modeling results remained significant after adjusting for sex, age, lifestyle factors,

BMI, and statin treatment. The individual BCP assessment showed that within the same sex, age, and BMI group (normal weight, overweight, and obesity), a variety of individual BCPs were found, exhibiting different combinations of predicted disease probabilities (Figure 3). Taken together, these findings stress the importance of a multivariable approach investigating associations between fat distribution and metabolic diseases. Different diseases were linked to different BCPs, or imbalances in fat accumulation, which could not be described by sex, age, lifestyle, or generalized adiposity or by investigating a single fat compartment alone.

Context of current literature

VATi was identified as a key variable in understanding metabolic diseases. For CHD, this is concurrent with prospective findings from, for example, the Dallas Heart Study (2) and Framingham Heart Study (12), showing associations between elevated VAT and increased cardiovascular risk factors and incidence of cardiovascular events. For T2D, our results agree with those from the Cooperative Health Research in the Augsburg Region (KORA) MRI study (24), in which significantly higher VAT and liver fat were found among diabetics and prediabetics without previous cardiovascular problems. These differences remained significant after correction for sex, age, systolic blood pressure, smoking status, high-density lipoprotein and low-density lipoprotein cholesterol levels, and triglyceride levels.

The results associating liver PDFF to T2D are well aligned with previously observed associations to the development of diabetes (22). However, for liver fat and CHD, the picture is more complex. There are many studies that have linked hepatic steatosis to cardiovascular disease (33–35) as well as recent studies that have reported elevated liver fat as not having a significant association to CHD after BMI adjustment.

TABLE 2 Descriptive statistics and results on coronary heart disease and type 2 diabetes

	Disease group	All controls	Matched controls	Matched controls + BMI
Coronary heart disease				
N subjects	237	4,400	237	237
Age, y	67.61 (62.78-71.22)	61.56 (55.14-67.07)	67.61 (62.79-71.23)	67.50 (63.09-71.14)
Sex, male/female	165/72	1,838/2,562	165/72	165/72
Weight, kg	80.80 (71.20-90.85)	73.00 (64.00-83.80)	78.00 (69.60-86.10) ^a	81.30 (72.00-91.30)
BMI, kg/m²	27.52 (24.98-30.53)	25.64 (23.25-28.48)	26.32 (23.83-28.85) ^b	27.45 (24.97-30.47)
Physical activity, MET-min/wk	3,498.62 (1,520.19-5,901.56)	3,579.75 (1,878.50-6,101.81)	3,819.75 (2,065.75-6,382.50)	3,449.19 (1,872.94-6,715.00) ^c
Smoking status, never/previous/current	115/100/16	2,762/1,439/188	142/87/7 ^d	126/106/4
Alcohol intake, g/d	16.14 (5.96-29.30)	15.80 (7.10-27.36)	18.77 (9.04-31.94) ^c	18.43 (8.93-32.41)
Statins medication, %	81.013	0.5	0.844 ^e	0.422 ^e
Visceral adipose tissue, L	4.71 (2.95-6.66)	2.94 (1.73-4.41)	3.89 (2.45-5.56) ^b	4.32 (2.72-6.16)
Abdominal subcutaneous adipose tissue, L	6.57 (4.85-8.89)	6.32 (4.64-8.54)	5.98 (4.41-8.02) ^c	6.50 (4.77-9.46)
Thigh muscle volume, L	11.04 (8.93-12.57)	9.47 (8.02-12.03)	11.27 (9.09-12.76)	11.48 (9.00-13.00)
Weight-to-muscle ratio, kg/L	7.51 (6.68-8.49)	7.43 (6.59-8.41)	7.04 (6.43-7.91) ^a	7.21 (6.52-8.42)
Liver proton density fat fraction, %	2.69 (1.64-7.39)	2.15 (1.40-3.95)	2.53 (1.55-5.08)	2.89 (1.77-5.84)
Fat ratio, %	52.32 (44.84-59.37)	49.34 (41.24-57.18)	47.88 (40.70-55.71) ^b	50.03 (41.68-59.29)
Visceral abdominal adipose tissue index, L/m²	1.72 (1.08-2.24)	1.05 (0.63-1.55)	1.29 (0.83-1.85) ^b	1.48 (0.97-2.06) ^c
Abdominal subcutaneous adipose tissue index, L/m²	2.21 (1.70-3.07)	2.21 (1.59-3.12)	1.99 (1.47-2.92) ^a	2.16 (1.55-3.30)
Total abdominal adipose tissue index, L/m²	4.14 (3.01-5.33)	3.39 (2.49-4.54)	3.36 (2.60-4.68) ^b	3.89 (2.85-5.23)
Muscle fat infiltration, %	7.82 (6.55-9.33)	7.07 (6.08-8.21)	7.32 (6.27-8.16) ^b	7.49 (6.31-8.89)
Type 2 diabetes				
N subjects	279	5,704	279	279
Age, y	65.57 (60.99-70.44)	62.99 (56.34-68.05)	65.57 (60.99-70.43)	65.75 (61.13-70.49)
Sex, male/female	183/96	2,669/3,035	183/96	183/96
Weight, kg	85.55 (77.12-98.92)	74.40 (65.20-85.10)	77.90 (68.62-88.75) ^b	87.50 (75.55-98.40)
BMI, kg/m²	29.51 (26.54-33.44)	25.99 (23.54-28.85)	26.56 (24.15-28.91) ^b	29.48 (26.59-33.38)
Physical activity, MET-min/wk	2,475.75 (1,102.81-4,597.31)	3,543.75 (1,853.59-6,061.50)	3,790.88 (1,940.23-5,851.69) ^a	3,097.44 (1,629.00-5,768.56)
Smoking status, never/previous/current	141/123/12	3,435/1,954/248	164/98/13	148/120/9
Alcohol intake, g/d	10.98 (2.63-23.35)	15.80 (7.20-28.40)	16.14 (7.90-30.80) ^b	17.04 (7.90-35.89) ^b
Statins medication, %	69.176	18.145	25.806 ^e	28.674 ^e
Visceral adipose tissue, L	5.90 (3.95-7.72)	3.24 (1.91-4.88)	3.68 (2.28-5.42) ^b	5.20 (3.62-7.19) ^c
Abdominal subcutaneous adipose tissue, L	7.75 (5.68-10.54)	6.38 (4.73-8.54)	6.05 (4.38-8.25) ^b	7.58 (5.64-10.87)
Thigh muscle volume, L	10.86 (9.15-12.66)	9.81 (8.11-12.24)	11.21 (8.55-12.96)	11.51 (9.31-13.37) ^c
Weight-to-muscle ratio, kg/L	7.81 (7.04-8.94)	7.40 (6.62-8.41)	7.13 (6.44-8.03) ^b	7.56 (6.74-8.95) ^c
Liver proton density fat fraction, %	6.51 (2.69-12.82)	2.29 (1.46-4.28)	2.43 (1.61-4.88) ^b	3.70 (2.09-7.53) ^b
Fat ratio, %	56.14 (48.61-63.37)	49.82 (41.93-57.42)	49.21 (40.37-55.73) ^b	53.68 (46.41-62.53)
Visceral abdominal adipose tissue index, L/m²	2.04 (1.45-2.60)	1.14 (0.69-1.67)	1.29 (0.79-1.87) ^b	1.78 (1.27-2.37) ^a
Abdominal subcutaneous adipose tissue index, L/m²	2.70 (1.87-3.72)	2.21 (1.62-3.11)	2.01 (1.45-2.86) ^b	2.60 (1.87-3.90)
Total abdominal adipose tissue index, L/m²	4.82 (3.76-6.32)	3.50 (2.59-4.62)	3.41 (2.57-4.50) ^b	4.57 (3.36-6.03)
Muscle fat infiltration, %	8.35 (6.96-9.87)	7.15 (6.15-8.35)	7.16 (6.10-8.38) ^b	7.75 (6.49-9.24) ^a

For continuous variables, median and interquartile range shown.

Matched controls are sex-and-age matched; matched controls + BMI are additionally matched on BMI.

^a*P* < 0.01.

^b*P* < 0.001.

^c*P* < 0.05 (two-sample *t* test).

^d*P* < 0.05.

^e*P* < 0.001 (Mann-Whitney *U* test).

MET, metabolic equivalents.

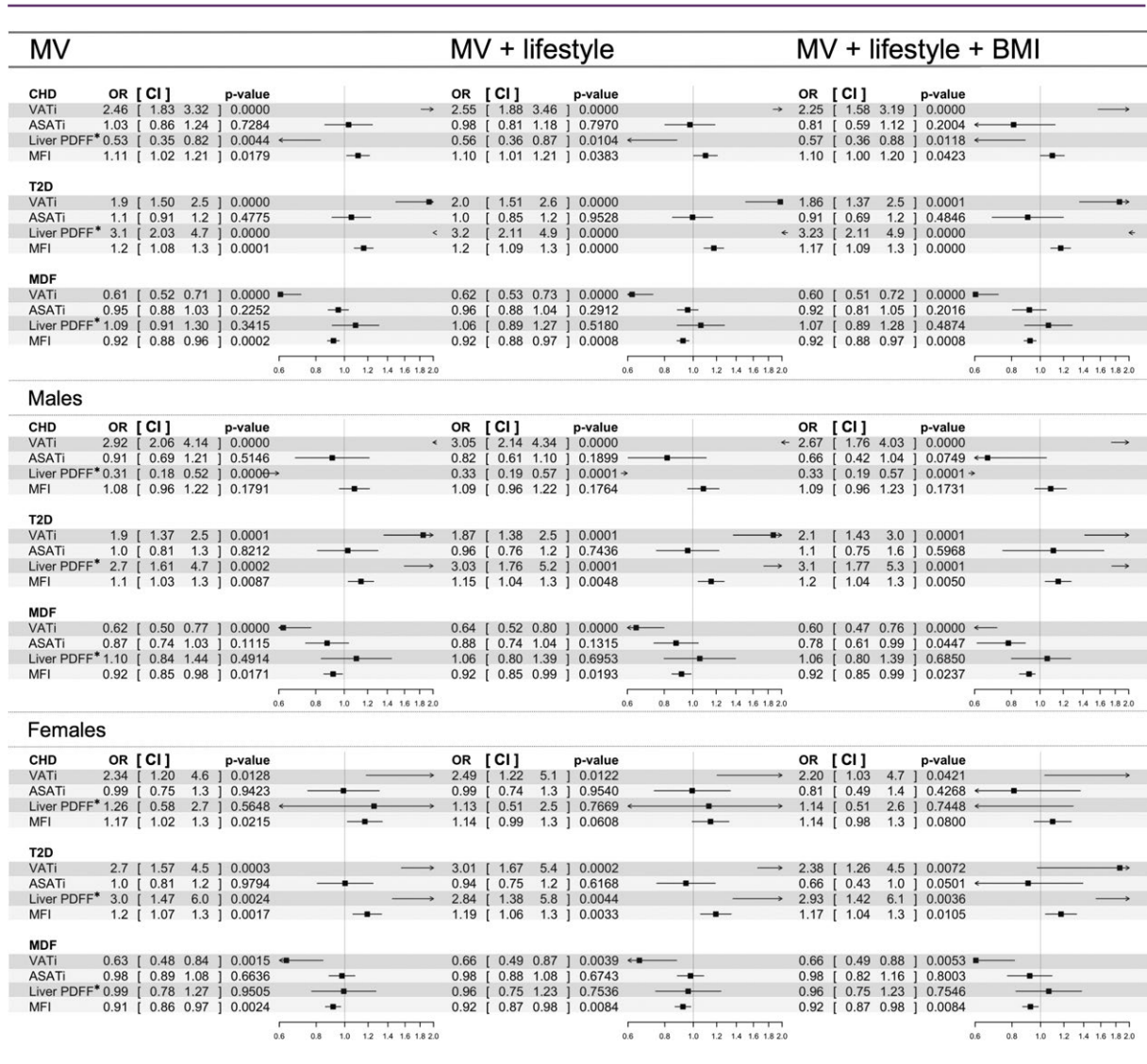


Figure 5 Results from the multivariable statistical modeling of coronary heart disease, type 2 diabetes, and metabolic disease free. Odds ratios and associated confidence intervals are shown with values and in forest plots. Black boxes indicate odds ratio value, horizontal lines the width of the confidence interval, and the vertical dashed line the line of null effect. Arrows are shown where confidence intervals are exceeding axis limits. MV model was adjusted for sex (whole cohort model only) and age. MV + lifestyle was additionally adjusted for smoking status, alcohol intake, and physical activity. MV + lifestyle + BMI was additionally adjusted for BMI. *Liver PDFF normalized using Box-Cox transform. ASATi, abdominal adipose tissue index; CHD, coronary heart disease; CI, confidence interval; PDFF, proton density fat fraction; MDF, metabolic disease free; MFI, muscle fat infiltration; OR, odds ratio; T2D, type 2 diabetes; VATi, visceral adipose tissue index.

However, there are few studies that have investigated liver fat as one among multiple body composition biomarkers describing fat accumulation. Another is the Dallas Heart Study, showing the importance of VAT and no association of cardiovascular events to liver fat after correction for BMI or VAT (2). Important differences comparing this study and the present is that it only included subjects with obesity and, possibly, too few cases to reveal multivariable associations. A recent large study investigating long-term outcomes in patients with biopsy-proven non-alcoholic fatty liver disease (NAFLD) showed no significant difference in cardiovascular death comparing NAFLD cases with controls (36). However, this study did not include other fat compartments, leaving multivariable associations unknown.

Lower liver PDFF among those who have experienced a cardiac event, as compared with controls, might be caused by subsequent disease treatment, or it could be an indication that a phenotype exists exhibiting a body composition with skewed fat accumulation that is associated with diagnosed CHD or common CHD comorbidities, such as chronic liver disease. The nonsignificant association between liver PDFF and CHD observed in females might be because of the lower prevalence of CHD among females, or that females rarely exhibit the skewness in fat accumulation driving the negative association between liver PDFF and CHD for the males. The observed finding of liver PDFF being negatively associated with CHD was not a direct effect of statin treatment. Prospective data can demonstrate potential causality and predictive value of this finding.

Associations of MFI to metabolic risk factors have previously been reported from the Framingham Heart Study (37). MFI has also been reported to be associated with insulin resistance in obesity and T2D (21). Our study showed a negative association between MFI and MDF and a positive association to T2D. However, associations between CHD and MFI were different in the sex-stratified analyses; they were not significant for males and were significant, or borderline significant, for females depending on correction factors. Although the Framingham Heart Study (37) did adjust for VAT, the approach of measuring MFI was not the same.

The individual BCP assessment (Figure 3) showed subjects with obesity with lower disease probability compared with subjects with normal weight, adding to the literature on healthy obesity (38-40). It was further strengthened by the comparison between the subject with normal weight with inflated BCP (Figure 3, top right) and the subject with obesity and a more star-shaped BCP (Figure 3, bottom left). This comparison yields a predicted probability for CHD and T2D with a factor 2 higher for the subject with normal weight and a factor 0.5 lower for MDF. That BMI has limitations in describing the individual is no longer a controversial statement, and the existence of body compositions in subjects with high BMI that are not disadvantageous from a health perspective has become more accepted in current literature. However, the results from the individual assessment yield a much more complex picture. Within all BMI classes, a range of BCPs were found, some of which associated with MDF, others with only CHD, only T2D, or those exhibiting comorbid disease association. Individuals exhibiting high predicted probability for MDF (Figure 3, first column) had BCPs more similar to the MDF group, represented by the reference star. Individuals exhibiting high predicted probability for CHD but low for T2D (Figure 3, second column) seemed to be characterized by high VAT_i and MFI but low liver PDFF. Individuals exhibiting high predicted probability for T2D but low for CHD (Figure 3, third column) seemed to be characterized by high VAT_i and liver PDFF but low MFI. Finally, individuals exhibiting comorbid disease association (Figure 3, fourth column) were characterized by high VAT_i, liver PDFF, and MFI. Although these subjects are among the extremes on the spectrum of combined predicted probabilities for CHD and T2D (i.e., low-low, high-low, low-high, high-high), they exemplify the diversity in disease associations to multivariable body composition. This emphasizes the importance of centering the analyses around the individuals, something rarely, if ever, seen in the body composition literature.

Implications

This study showed the complexity in investigating disease associations to fat distribution and the importance of a multivariable approach. With the identification of specific fat distributions associated with different diseases, more targeted and effective disease treatments could be developed. Furthermore, a multivariable description of an individual's body composition, attained from a single examination, enables a more standardized and detailed description of a patient's metabolic disease status. By combining multivariable body composition analysis with already measured biomarkers, there is potential for highly individualized intervention plans.

Body composition profiling and visualization allowed for a quick and simultaneous assessment of an individual's or group's fat accumulation pattern, fat and muscle distribution, and balance between adipose tissue

compartments. The visualization introduces the possibility to easily distinguish between different phenotypes in a multivariable space. The star-shaped reference effectively shapes the BCP to highlight the ectopic fat compartments, and a quick assessment, based on current knowledge, of an individual's risk profile can be made.

Our study makes significant advances to current literature by presenting normative values of standardized body composition parameters for metabolic health and disease (CHD and T2D) (Table 1 and Table 2). This brings context of high importance to future studies investigating body composition and metabolic disease.

The broad use of MRI to assess body composition has thus far not been possible because of limitations in cost and access. Sources of cost are, for example, the scanning time and laborious manual segmentation of anatomical regions. In UK Biobank, a 6-minute protocol was implemented for the complete body composition assessment, and the combination with advanced image analysis techniques enabled automatic segmentations of anatomical regions and extraction of biomarker values. Today, this is a solution available also outside the image processing research community. The short acquisition protocol and automated image analysis enable cost-effective assessment of patients with suspected metabolic-related diseases, such as NAFLD, chronic liver disease, or cardiovascular disease. In particular, this technique can be easily added to provide further metabolic disease profiling of such patients that are already examined using MRI.

Strengths and limitations

This study utilized measurements with high reproducibility, accuracy, and precision describing fat distribution gathered on a large number of well-characterized subjects. The technique has been validated on many different MRI scanners, and the standardization of measures allows comparisons across and between large cohorts. Simultaneous inclusion of several body composition measures strengthened the investigation of disease associations to adipose tissue distribution. Furthermore, in terms of disease information, we benefitted from the integration of self-reported and diagnosis data from electronic health care records.

There are some limitations. First, this study was based on cross-sectional data, and medications taken into account included only statins and not the time on medication. This leaves the causality and predictive power of the BCP unknown. Future analyses should focus on additional medications that may affect liver fat or adiposity. Second, self-reported data were used to control for confounding effects and in disease definitions. Future availability of biochemical assays and primary care data enables a more detailed investigation of the metabolic syndrome. Thirdly, there is evidence of UK Biobank exhibiting a "healthy volunteer" selection bias (41). However, conclusions on associations between exposures and health outcomes are generalizable to the wider population because of the large sample size and heterogeneity of exposure measures (41). Also, the bias was partly amended by correcting for general adiposity and lifestyle factors. When more subjects have been scanned, further investigations can be made, including other ethnicities, age ranges, and sociodemographic factors. Lastly, our study investigated the associations between multivariable body composition and metabolic diseases, showing associations mainly to VAT_i, MFI, and liver PDFF. Investigating other areas of disease may instead reveal the importance of other variables, including lean muscle volume, total fat, and weight, WMR, FR, ASAT_i, and TAAT_i.

Conclusion

Body composition profiling enabled an intuitive visualization of body composition and showed the complexity of associations between fat distribution and different metabolic diseases on both population and individual levels, stressing the importance of a multivariable approach. The analyses showed unique associations to diagnosed CHD, T2D, and MDF. VATi and MFI were negatively associated with MDF, and higher values were observed in CHD and T2D. The associations of liver fat were ambiguous; they were negative with CHD, positive with T2D, and nonsignificant with MDF. This could not be described by sex, age, lifestyle, or generalized adiposity or by investigating a single fat compartment alone. Altogether, multivariable body composition profiling showed the potential to improve the description of the interplay between different adipose tissue compartments, ectopic fat accumulation, and metabolic disease profiles. **O**

© 2018 The Authors. *Obesity* published by Wiley Periodicals, Inc. on behalf of The Obesity Society (TOS)

References

1. Prentice AM, Jebb SA. Beyond body mass index. *Obes Rev* 2001;2:141-147.
2. Neeland IJ, Turer AT, Ayers CR, et al. Body fat distribution and incident cardiovascular disease in obese adults. *J Am Coll Cardiol* 2015;65:2150-2151.
3. Tomiyama AJ, Hunger JM, Nguyen-Cuu J, Wells C. Misclassification of cardiometabolic health when using body mass index categories in NHANES 2005-2011. *Int J Obes (Lond)* 2016;40:883-886.
4. Thomas EL, Fitzpatrick JA, Malik SJ, Taylor-Robinson SD, Bell JD. Whole body fat: content and distribution. *Prog Nucl Magn Reson Spectrosc* 2013;73:56-80.
5. Schlett CL, Hendel T, Weckbach S, et al. Population-based imaging and radiomics: rationale and perspective of the German National Cohort MRI Study. *Rofa* 2016;188:652-661.
6. Bamberg F, Hetterich H, Rospleszcz S, et al. Subclinical disease burden as assessed by whole-body MRI in subjects with prediabetes, subjects with diabetes, and normal control subjects from the general population: The KORA-MRI Study. *Diabetes* 2017;66:158-169.
7. West J, Dahlqvist Leinhard O, Romu T, et al. Feasibility of MR-based body composition analysis in large scale population studies. *PLoS ONE* 2016;11:e0163332. doi:10.1371/journal.pone.0163332
8. Cruz-Jentoft AJ, Baeyens JP, Bauer JM, et al. Sarcopenia: European consensus on definition and diagnosis: report of the European Working Group on Sarcopenia in Older People. *Age Aging* 2010;39:412-423.
9. Borga M, Thomas EL, Romu T, et al. Validation of a fast method for quantification of intra-abdominal and subcutaneous adipose tissue for large scale human studies. *NMR Biomed* 2015;28:1747-1753.
10. Demerath EW, Reed D, Rogers N, et al. Visceral adiposity and its anatomical distribution as predictors of the metabolic syndrome and cardiometabolic risk factor levels. *Am J Clin Nutr* 2008;88:1263-1271.
11. Britton KA, Fox CS. Ectopic fat depots and cardiovascular disease. *Circulation* 2011;124:e837-e841.
12. Lee JJ, Pedley A, Hoffmann U, Massaro JM, Fox CS. Association of changes in abdominal fat quantity and quality with incident cardiovascular disease risk factors. *J Am Coll Cardiol* 2016;68:1509-1521.
13. Liu J, Fox CS, Hickson DA, et al. Impact of abdominal visceral and subcutaneous adipose tissue on cardiometabolic risk factors: The Jackson Heart Study. *J Clin Endocrinol Metab* 2010;95:5419-5426.
14. Neeland IJ, Ayers CR, Rohatgi AK, et al. Associations of visceral and abdominal subcutaneous adipose tissue with markers of cardiac and metabolic risk in obese adults. *Obesity (Silver Spring)* 2013;21:e439-e447.
15. Kurioka S, Murakami Y, Nishiki M, Sohmiya M, Koshimura K, Kato Y. Relationship between visceral fat accumulation and anti-lipolytic action of insulin in patients with type 2 diabetes mellitus. *Endocr J* 2002;49:459-464.
16. Iwasa M, Mifuji-Moroka R, Hara N, et al. Visceral fat volume predicts new-onset type 2 diabetes in patients with chronic hepatitis C. *Diabetes Res Clin Pract* 2011;94:468-470.
17. van der Poorten D, Milner KL, Hui J, et al. Visceral fat: a key mediator of steatohepatitis in metabolic liver disease. *Hepatology* 2008;48:449-457.
18. Doyle SL, Donohoe CL, Lysaght J, Reynolds JV. Visceral obesity, metabolic syndrome, insulin resistance, and cancer. *Proc Nutr Soc* 2012;71:181-189.
19. Britton KA, Massaro JM, Murabito JM, Kreger BE, Hoffmann U, Fox CS. Body fat distribution, incident cardiovascular disease, cancer, and all-cause mortality. *J Am Coll Cardiol* 2013;62:921-925.
20. Marcus RL, Addison O, Dibble LE, Foreman KB, Morrell G, Lastayo P. Intramuscular adipose tissue, sarcopenia, and mobility function in older individuals. *J Aging Res* 2012;2012:629637. doi:10.1155/2012/629637
21. Goodpaster BH, Thaete FL, Kelley DE. Thigh adipose tissue distribution is associated with insulin resistance in obesity and in type 2 diabetes mellitus. *Am J Clin Nutr* 2000;71:885-892.
22. Ekstedt M, Franzén LE, Mathiesen UL, et al. Long-term follow-up of patients with NAFLD and elevated liver enzymes. *J Hepatol* 2006;44:865-873.
23. Wattacheril J, Chalasani N. Nonalcoholic fatty liver disease (NAFLD): is it really a serious condition? *J Hepatol* 2012;56:1580-1584.
24. Bamberg F, Hetterich H, Rospleszcz S, et al. Subclinical disease burden as assessed by whole-body mri in subjects with prediabetes, subjects with diabetes, and normal control subjects from the general population: The KORA-MRI Study. *Diabetes* 2017;66:158-169.
25. UK Biobank Imaging Study. <http://imaging.ukbiobank.ac.uk>. Accessed September 17, 2017.
26. Sudlow C, Gallacher J, Allen N, et al. UK Biobank: an open access resource for identifying the causes of a wide range of complex diseases of middle and old age. *PLoS Med* 2015;12:e1001779. doi:10.1371/journal.pmed.1001779
27. Leinhard OD, Johansson A, Rydell J, et al. Quantitative abdominal fat estimation using MRI. Presented at: Proceedings of the 19th International Conference on Pattern Recognition (ICPR); December 8-11, 2008; Tampa, FL. doi:10.1109/ICPR.2008.4761764
28. Karlsson A, Rosander J, Romu T, et al. Automatic and quantitative assessment of regional muscle volume by multi-atlas segmentation using whole-body water-fat MRI. *J Magn Reson Imaging* 2015;41:1558-1569.
29. West J, Romu T, Thorell S, et al. Precision of MRI-based body composition measurements of postmenopausal women. *PLoS One* 2018;13:e0192495. doi:10.1371/journal.pone.0192495
30. Heymsfield SB, Gallagher D, Mayer L, Beetsch J, Pietrobelli A. Scaling of human body composition to stature: new insights into body mass index. *Am J Clin Nutr* 2007;86:82-91.
31. UK Biobank data showcase. UK Biobank website. <http://biobank.ctsu.ox.ac.uk/crystal/>. Accessed November 16, 2017.
32. Neuraz A, Chochana L, Malamut G, et al. Phenome-wide association studies on a quantitative trait: application to TPMT enzyme activity and thiopurine therapy in pharmacogenomics. *PLoS Comput Biol* 2013;9:e1003405. doi:10.1371/journal.pcbi.1003405
33. Targher G, Arcaro G. Non-alcoholic fatty liver disease and increased risk of cardiovascular disease. *Arteriosclerosis* 2007;191:235-240.
34. Brea A, Pintó X, Ascaso JF, et al. Review article: nonalcoholic fatty liver disease, association with cardiovascular disease and treatment. (I). Nonalcoholic fatty liver disease and its association with cardiovascular disease. *Clin Investig Arterioscler* 2017;29:141-148.
35. Hamaguchi M, Kojima T, Takeda N, et al. Nonalcoholic fatty liver disease is a novel predictor of cardiovascular disease. *World J Gastroenterol* 2007;13:1579-1584.
36. Hagström H, Nasr P, Ekstedt M, et al. Fibrosis stage but not NASH predicts mortality and time to development of severe liver disease in biopsy-proven NAFLD. *J Hepatol* 2017;67:1265-1273.
37. Therkelsen KE, Pedley A, Speliotes EK, et al. Intramuscular fat and associations with metabolic risk factors in the framingham heart study. *Arterioscler Thromb Vasc Biol* 2013;33:863-870.
38. Després JP. Obesity and cardiovascular disease: weight loss is not the only target. *Can J Cardiol* 2015;31:216-222.
39. Thomas EL, Parkinson JR, Frost GS, et al. The missing risk: MRI and MRS phenotyping of abdominal adiposity and ectopic fat. *Obesity (Silver Spring)* 2012;20:76-87.
40. Arsenaault BJ, Lachance D, Lemieux I, et al. Visceral adipose tissue accumulation, cardiorespiratory fitness, and features of the metabolic syndrome. *Arch Intern Med* 2007;167:1518-1525.
41. Fry A, Littlejohns TJ, Sudlow C, et al. Comparison of sociodemographic and health-related characteristics of UK Biobank participants with the general population. *Am J Epidemiol* 2017;186:1026-1034.